# Variations in Steady-State and Time-Resolved Background Luminescence from Surface-Enhanced Resonance Raman Scattering-Active Single Ag Nanoaggregates

**Tamitake Itoh,*,† Yasuo Kikkawa,‡ Vasudevanpillai Biju,† Mitsuru Ishikawa,† Akifumi Ikehata,‡ and Yukihiro Ozaki‡**

*Nano-Bioanalysis Team, Health Technology Research Center, National Institute of Advanced Industrial Science and Technology (AIST), 2217-14 Hayashi-cho, Takamatsu Kagawa 761-0395, Japan, and Department of Chemistry, School of Science and Technology, Kwansei Gakuin University, Sanda, Hyogo 669-1337, Japan*

*Received: June 29, 2006; In Final Form: September 4, 2006*

We observed a background luminescence emission that was associated with surface-enhanced resonance Raman scattering (SERRS) of rhodamine 6G (R6G) molecules adsorbed on single Ag nanoaggregates and investigated the origin of the background luminescence. Thanks to the observation of single nanoaggregates, we clearly identified nanoaggregate-by-nanoaggregate variations in the steady-state and time-resolved background luminescence spectra of each nanoaggregate. From the variations in the steady-state spectra, two kinds of key properties were revealed. First, the background luminescence spectra were divided into four components: one fluorescence band corresponding to the monomers of R6G and three Lorentzian bands whose maxima were red-shifted from the fluorescence maximum of the monomer by several tens of nanometers. On the basis of the red-shifted luminescence maxima, and experimental and theoretical studies of background luminescence, we attributed the three background luminescences to fluorescence from aggregates (dimer and two kinds of higher-order aggregates) of R6G molecules on an Ag surface. Second, a positive correlation was observed between wavelengths of background luminescence maxima and wavelengths of plasmon resonance maxima. This positive correlation invoked the idea that the dipoles of both the background luminescence and the plasmon radiation are coupled with each other. From the key observations in the steady-state background luminescence spectra, we propose that two factors contribute to the variations in the steady-state background luminescence spectra; one is the aggregation (monomer, dimer, and two kinds of higher-order aggregates) of R6G molecules on an Ag surface, and the other is plasmon resonance maxima of single Ag nanoaggregates. Considering these two factors, we propose that the variations in the time-resolved background luminescence spectra are associated with deaggregation of R6G molecules (higher- to lower-order aggregates) and temporal shifts in the plasmon resonance maxima of single Ag nanoaggregates.

## Introduction

Enormous enhancement of resonance Raman scattering arises from molecules adsorbed on the surfaces of noble metal nanoaggregates. This phenomenon is widely known as SERRS. Indeed, SERRS has recently attracted great interest for applications in analytical science because of the enormous enhancement by a factor of $10^8$ to $10^{14}$ in SERRS. This enhancement advanced the detection limit of a wide variety of molecules from an ensemble to a single molecule level.[1−25] There is no doubt that EM fields that are coupled with plasmons of metal nanoaggregates mainly contribute to the enormous enhancement of SERRS.[5,21,22] Furthermore, the relationship between strong SERRS intensity and silver−nanoparticle microstructure/particle interactions was experimentally evidenced.[24,25] However, there are still ongoing issues on the mechanism of SERRS. One of the unsolved important characteristics of SERRS is the background luminescence that always appears along with SERRS but is absent in usual Raman scattering.[13−18,23] Thus, investigation of the background luminescence is important for us not only to understand the background luminescence property itself but also to elucidate a detailed mechanism of SERRS. The following five mechanisms are proposed to be the origin of the background luminescence: (i) Raman scattering of optically excited electron−hole pairs in the intrasurface band of metals by the phonons;[26−28] (ii) electronic Raman scattering from a metal surface defects caused by exchanging electrons between adsorbed molecules and a metal surface; (iii) luminescence due to recombination of holes in a d band and electrons in a sp conduction band of noble metals;[18,23,29−39] (iv) fluorescence of physisorbed molecules on metal surfaces; (v) and fluorescence of chemisorbed molecules on metal surfaces. To trace the origin of the background luminescence from SERRS-active metal nanoaggregates, we previously developed an experimental setup for light scattering microspectroscopy[40,41] and demonstrated using single Ag nanoaggregates adsorbed with R6G molecules that (i) SERRS-inactive Ag nanoaggregates do not show luminescence under SERRS excitation intensities of several tens to hundreds milliwatts per square centimeter; (ii) luminescence maxima are independent of the excitation wavelengths; (iii) the polarization of the background luminescence is the same as that of plasmon resonance Rayleigh scattering and SERRS; and (iv) intensities of SERRS and the background luminescence are proportional to the quality factor $Q$ of a plasmon resonance band.[42] The results (i−iv) favor the idea that the background luminescence is attributed to fluorescence of R6G molecules

* Corresponding author. E-mail: tamitake-itou@aist.go.jp.
† National Institute of Advanced Industrial Science and Technology.
‡ Kwansei Gakuin University.

10.1021/jp064070p CCC: $33.50 
Published on Web 10/11/2006

physisorbed or chemisorbed on a metal surface; however, the results argue against the idea of Raman scattering from optically excited electron−hole pairs in the intrasurface bands of metals, electronic Raman scattering from Ag surface defects, and luminescence due to recombination of holes and electrons.

From the results of (iii) and (iv), we infer that the plasmon is coupled with both SERRS and background luminescence. Here, we have a theoretical model that associates plasmon with the enhancement of both the Raman scattering and the background luminescence.[43] This theoretical model predicts that dipole−dipole coupling between electronic resonance of a molecule, and plasmon resonance of a metal nanoparticle plays an important role in the enhancement of both the Raman scattering and the background luminescence. Note that the metal nanoparticle dipole in ref 41 is equivalent to a plasmon dipole. In the theoretical model, SERRS was treated as a scattering process including 2-fold dipole−dipole interactions in the following five steps:[43] (i) an incident photon $h\omega_i$ is absorbed by a metal nanoparticle (M); (ii) the absorbed photon is nonradiatively scattered to a molecule (D) mediated by dipole−dipole coupling; (iii) a part of the absorbed photon energy is converted into a Raman scattering photon; (iv) the Raman scattering photon is nonradiatively scattered back from D to M mediated by the dipole−dipole coupling; and (v) the photon $h\omega_{sc}$ that is nonradiatively scattered twice in (ii) and (iv) is radiatively scattered as Raman scattering to the far-field mediated by the plasmon−dipole radiation: $h\omega_i + (M/D) \rightarrow (M_{\omega i}*/D) \rightarrow (M/D_{\omega i}*) \rightarrow (M/D_{\omega sc}*) \rightarrow (M_{\omega sc}*/D) \rightarrow (M/D) + h\omega_{sc}$. Here, M/D represents a complex formed by the adsorption of a molecule on a metal nanoparticle, $h\omega_i$ and $h\omega_{sc}$ denote incident and Raman scattering photon energies, and the asterisk denotes the electronic excited state. Absorption and scattering of a photon by the metal nanoparticle in steps (i) and (v), each of which contributed to the enhancement of the incident and the scattered light, respectively, enlarge the effective cross-section of the Raman scattering. The 2-fold dipole−dipole interaction implies that photon energy stored in electronically excited molecules was transferred into a metal nanoparticle by dipole−dipole coupling, thereby suggesting a possibility that the molecule emits luminescence coupled with plasmon−dipole radiation.[43,44] On the basis of this possibility, we consider that the background luminescence maxima are associated with the plasmon resonance maxima. However, plasmon resonance maxima strongly depend on the size and shape of metal nanoaggregates and the dielectric property of the surrounding media.[45−50] Thus, the expected spectral association is smeared over an ensemble of nanoaggregates due to inhomogeneous spectral broadening of the plasmon resonance maxima. Therefore, nanoaggregate-by-nanoaggregate measurements on single metal nanoaggregates are essential to excluding spectral inhomogenity.[40−42]

In the current work, we investigated nanoaggregate-by-nanoaggregate variations in the background luminescence spectra from single SERRS-active Ag nanoaggregates adsorbed with R6G molecules to explore the mechanism of the background luminescence and made key observations in the steady-state and time-resolved background luminescence spectra to understand the origin of the variations. In the steady-state background luminescence spectra, we found that each spectrum was divided into four components: one fluorescence band of the R6G monomer and three Lorentzian bands whose maxima were red-shifted from the monomer fluorescence maximum by several tens of nanometers. We also observed positive correlations between wavelengths of the background luminescence maxima and the plasmon resonance maxima. In the time-resolved background luminescence spectra, we found that a background luminescence spectrum with multiple peaks temporally changed its maximum from one to another, and we observed simultaneous blue-shifts of both the background luminescence and the plasmon resonance maxima.

From a comparison of the observed spectral maxima of the background luminescence with those in previous reports of aggregated R6G molecules,[6,51−57] we attributed the background luminescence to the fluorescence of adsorbed R6G monomers and three kinds of aggregates: a dimer and two kinds of higher-order aggregates of R6G molecules adsorbed on Ag nanoaggregates. From the observed positive correlation, we attributed the variations in the background luminescence maxima to variations in the plasmon resonance maxima. Thus, we attributed the variations in the steady-state background luminescence maxima to variations in both aggregation of adsorbed R6G molecules (monomers, dimers, and two kinds of higher-order aggregates) and plasmon resonance maxima of single Ag nanoaggregates. Accordingly, we attributed the two kinds of variations in the time-resolved background luminescence spectra to temporal changes in the photoinduced deaggregation of adsorbed R6G aggregates (higher- to lower-order aggregates) and temporal blue-shifts of the plasmon resonance maxima, respectively. Additionally, we proposed a method of estimating the strength of the EM interaction between an Ag nanoaggregate and a SERRS-active R6G molecule from blue-shifts of the plasmon resonance maxima before and after SERRS quenching.

## Experimental Procedures

Details of our experimental setup for SERRS measurements are described elsewhere.[41] However, an outline of our experimental procedure in the present investigation is provided here. Ag nanoaggregates were prepared by incubating aqueous solutions containing R6G ($6.4 \times 10^{-9}$ M), NaCl (10 mM), and Ag colloid ($9.6 \times 10^{-11}$ M, ∼40 nm in diameter) for 5 min at room temperature (17 °C). This was followed by dispersing the Ag nanoaggregates on a glass plate by spin-coating at 3000 rpm. Excess dye molecules adsorbed on the glass plate were removed by rinsing with distilled water and acetone. The sample surface was covered with a several hundreds micrometer thick water layer. The Ag nanoaggregates were excited with either white light from a 50 W halogen lamp or a 532 nm circular polarized laser beam from an LD YAG second harmonics laser. The Ag nanoaggregates were irradiated at a laser flounce of 300 mW/cm$^2$. Excitation beams were introduced to the glass surface through a dark- and a bright-field condenser lens in an inverted optical microscope (IX70, Olympus, Tokyo). The plasmon resonance Rayleigh scattering and the SERRS plus background luminescence light from an isolated single Ag nanoaggregate were collected with an objective lens (LCPlanFl × 60, N.A. 0.7, Olympus, Tokyo). The collected light was introduced through a polychromator (Pro-275, Acton, Ottobrunn) into an electronically cooled charge-coupled device (DV434−FI, Andor, Tokyo). Collection integration time per one SERRS plus background luminescence spectrum was 5 s.

## Results

**SEM and Dark-Field Optical Images of Ag Nanoaggregates.** Figure 1A,B shows a representative plasmon resonance Rayleigh scattering image and a scanning electron microscope (SEM) image obtained from the same area of a glass plate on which Ag nanoaggregates were dispersed. Figure 1C shows enlarged SEM images, each of which corresponds to the

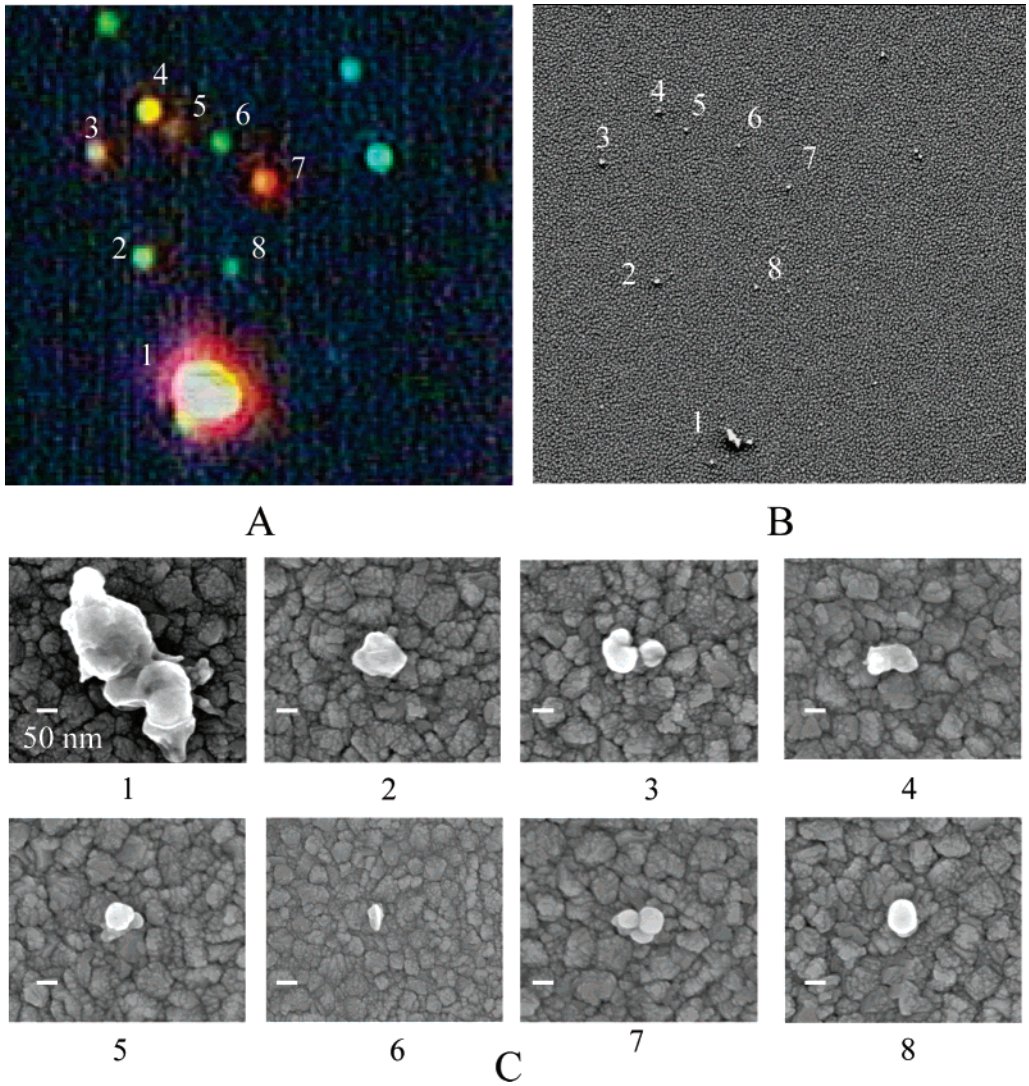


**Figure 1.** (A) Plasmon resonance Rayleigh scattering image and (B) scanning electron microscope (SEM) image of the same Ag nanoaggregates dispersed on a slide glass. (C) Enlarged SEM images of the Ag nanoaggregates that are numbered in panel B. Scale bars are all 50 nm.

numbered Ag nanoaggregates in Figure 1B. Figure 1A shows that the color of the Ag nanoaggregates varies from one nanoaggregate to another. The variations in the color are attributed to shape and size dependence of the plasmon resonance.[45−50] All the Ag nanoaggregates in Figure 1C are aggregates of several nanoparticles and are deviated from spherical shape. The white nanoaggregate indicated by number 1 in Figure 1A showed a complex Rayleigh scattering spectrum (figure not shown), which was associated with higher-order plasmon resonance. On the other hand, the simple colored nanoaggregates indicated by numbers 2−8 showed simple Rayleigh scattering spectra (figures not shown). Polarization dependence of their plasmon resonance bands was fitted to $\cos^2\theta$ curves (data not shown), thereby showing that the plasmons are dipolar.[8,45−50] In the current work, we selected SERRS-active Ag nanoaggregates that showed simple color, as shown in numbers 2−8 in Figure 1A. The selection of the simple color means that the selected SERRS-active nanoaggregates have a simple morphology and are composed of several Ag nanoparticles. This morphology is consistent with the observations of SERRS-active Ag nanoaggretates by atomic force microscopy (AFM) and SEM.[4,12−14,16,21,22] The key of the current work is the selection of the SERRS-active Ag nanoaggregates that show a dipolar plasmon resonance Rayleigh scattering spectrum. This selection was essential to elucidate direct correlation between the plasmon resonance maxima and the background luminescence maxima.

**Variations in the Steady-State Background Luminescence Spectra.** We identified variations in the steady-state background luminescence spectra of single SERRS-active Ag nanoaggregates. Figure 2A shows a fluorescence spectrum of R6G in an aqueous solution. Figure 2B−G shows representative steady-state background luminescence spectra from SERRS-active single Ag nanoaggregates. The dotted line in Figure 2B shows the fluorescence spectrum of R6G in an aqueous solution. Note that the leading edge of the fluorescence spectrum <540 nm was blocked by a 532 nm holographic notch filter. The highly structured bands observed around 550−580 nm in Figure 2B−G were attributed to SERRS bands.[6] The highly structured weak bands observed around 620−640 nm in Figure 2B−G were attributed to SERRS bands of combination and overtone modes.[6] The background luminescence spectra in Figure 2C−G showed multi-band structures. The background luminescence spectra were free from inhomogeneous broadening, otherwise present in ensample studies of multiple nanoaggregates, due to measurements on isolated single nanoaggregates. Thus, we assume that the background luminescence spectra are composed of Lorentzian bands. We divided each background luminescence spectrum in Figure 2C−G into one fluorescence band and three Lorentzian bands with maxima at 555, 580 ± 20, 620 ± 20, and 690 ± 20

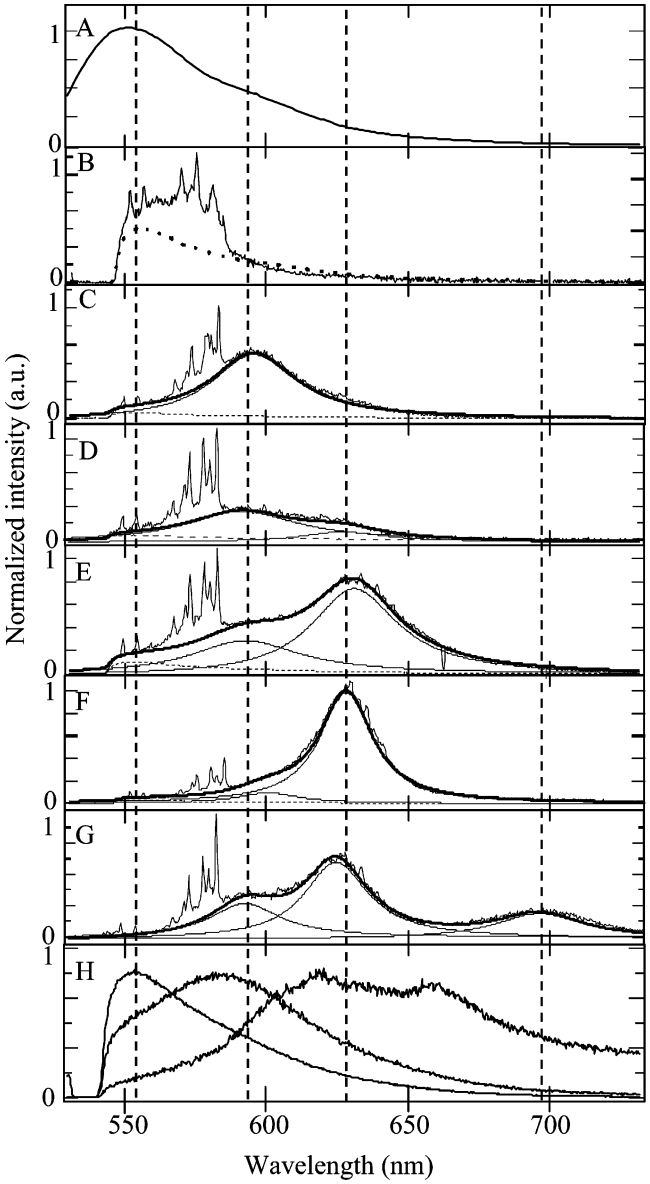


**Figure 2.** (A) Fluorescence spectrum of a R6G aqueous solution. (B−G) Representative background luminescence spectra from six isolated Ag nanoaggregates fitted with Lorentzian and fluorescence bands. Dotted line in panel B represents the fluorescence spectrum of an aqueous solution of R6G. Parameters of Lorentzian curves: (C) Lorentzian band with maximum $\lambda_{pk}$ of 590 nm (2.09 eV) and full width at half-maximum $\Gamma$ of 158 meV; (D) $\lambda_{pk}$s of 595 and 640 nm (2.09 and 1.98 eV) and $\Gamma$s of 150 and 117 meV; (E) $\lambda_{pk}$s of 593 and 632 nm (2.09 and 1.96 eV) and $\Gamma$s of 151 and 119 meV; (F) $\lambda_{pk}$s of 595 and 630 nm (2.10 and 1.97 eV) and $\Gamma$s of 149 and 123 meV; (G) $\lambda_{pk}$s of 593, 625, and 696 nm (2.09, 1.98, and 1.78 eV) and $\Gamma$s of 118, 95, and 87 meV. The highly structured bands observed around 550−580 nm in panels B−G are SERRS bands. (H) Fluorescence spectrum of aggregates of R6G on a glass plate. All the plots were normalized to intensities at spectral maxima.

nm, each of which is indicated by a vertical dashed line. Figure 2H shows fluorescence spectra of R6G aggregates prepared by evaporation of an R6G aqueous solution with a high concentration ($\sim 10^{-5}$ M) on a glass surface without the Ag colloid. Several kinds of broad bands with maxima distributed from 555 to 660 nm were observed.

**Correlation between the Background Luminescence Maxima and the Plasmon Resonance Maxima.** Figure 3A−F shows background luminescence bands plus SERRS bands, in solid lines, and plasmon resonance bands, in dashed lines, from

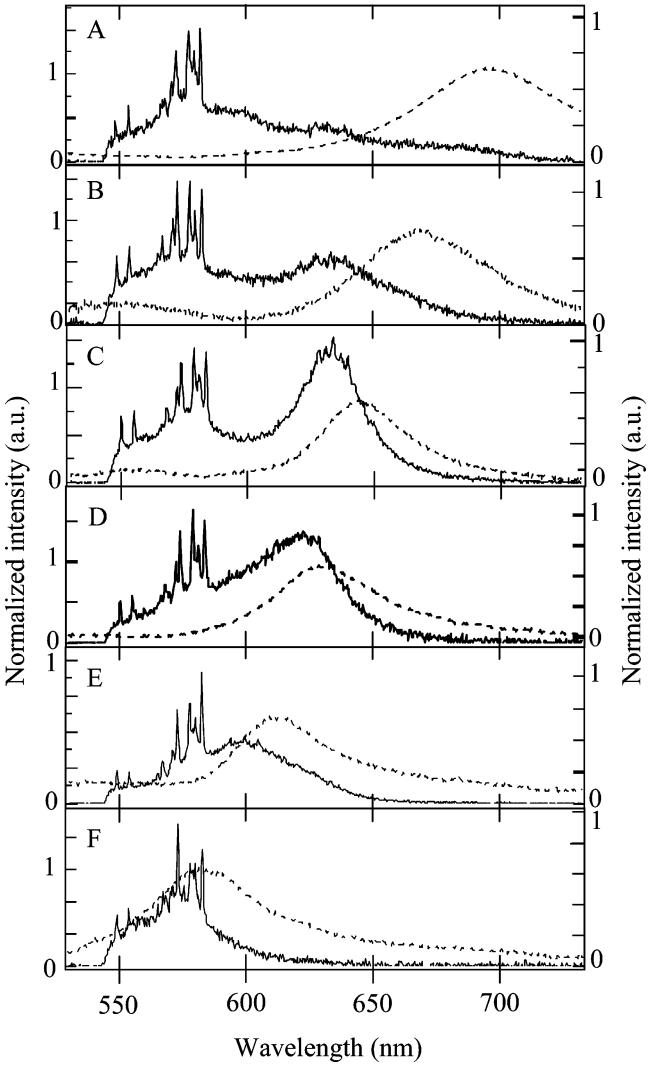


**Figure 3.** (A−F) Background luminescence bands (solid lines) and the corresponding plasmon resonance bands (dotted lines) of six single Ag nanoaggregates. All the plots were normalized to intensities at spectral maxima.

representative single SERRS-active Ag nanoaggregates. Note that the background luminescence and the plasmon resonance bands were measured for the same Ag nanoaggregate in each panel. We identified that the background luminescence maxima and the plasmon resonance maxima were different from nanoaggregate to nanoaggregate and that Ag nanoaggregates showing background luminescence maxima in the longer wavelength region also showed plasmon resonance maxima in the longer wavelength region. Figure 4 draws correlations between wavelengths of the background luminescence maxima and the plasmon resonance maxima for 40 single Ag nanoaggregates.

**Variations in the Time-Resolved Background Luminescence Spectra.** Temporal intermittence of SERRS and background luminescence was observed from one nanoaggregate to another in the current measurements. This intermittence is widely known as blinking.[1,2,9,12,14,16,20,21,23] From the preliminary experiments, we found a temporal change in the background luminescence spectra in addition to the blinking. To reveal a temporal change in the background luminescence spectra that is independent of blinking, we selectively measured the background luminescence without blinking. Figure 5A−D shows variations in the time-resolved background luminescence spectra of single SERRS-active Ag nanoaggregates, where time courses are indicated by arrows. From the time-resolved variations,

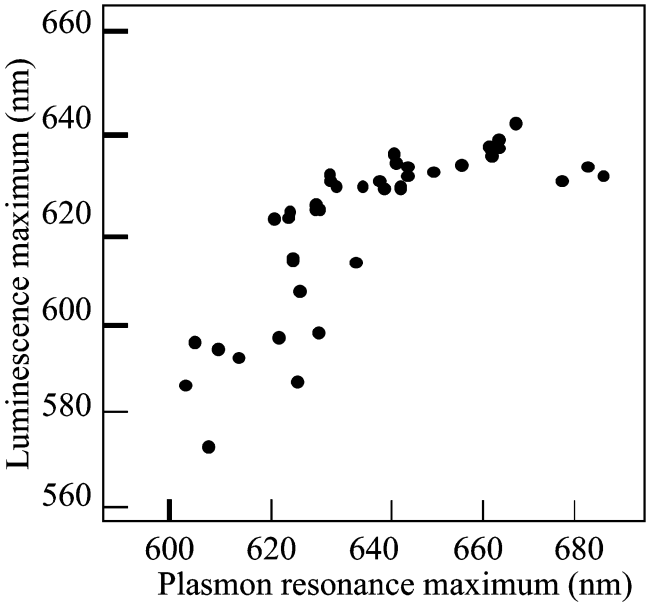


**Figure 4.** Wavelengths of background luminescence maxima vs wavelengths of plasmon resonance maxima for 40 single Ag nanoaggregates.

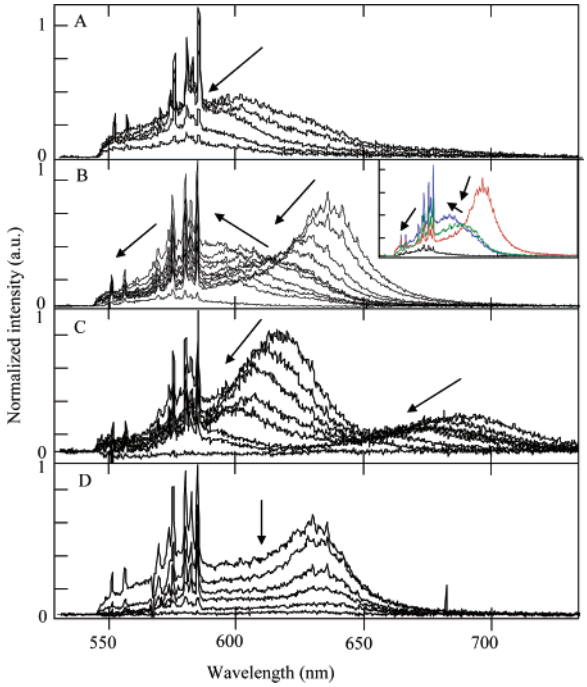


**Figure 5.** (A−D) Temporal variations in the background luminescence spectra of four single Ag nanoaggregates. Time course is indicated by the arrows. Three background luminescence spectra from Figure 5B are highlighted in the inset to make clear the temporal changes. It is necessary to write down the time at which the black, red, green, and blue spectra were recorded. All the plots were normalized to intensities at spectral maxima.

2-fold key observations were revealed: background luminescence maxima showing large blue-shifts by 20−80 nm correspond to Figure 5A−C, and those showing small changes by ±10 nm correspond to Figure 5D. Furthermore, we can highlight at least four observations of temporal variations in the background luminescence spectra: first, as shown in Figure 5A, a maximum at 600 nm blue-shifted by 20 nm with decrease of intensity; second, as shown in Figure 5B, a maximum at 635 nm blue-shifted by 25 nm with a decrease of intensity, and another maximum at 610 nm blue-shifted by 30 nm with an

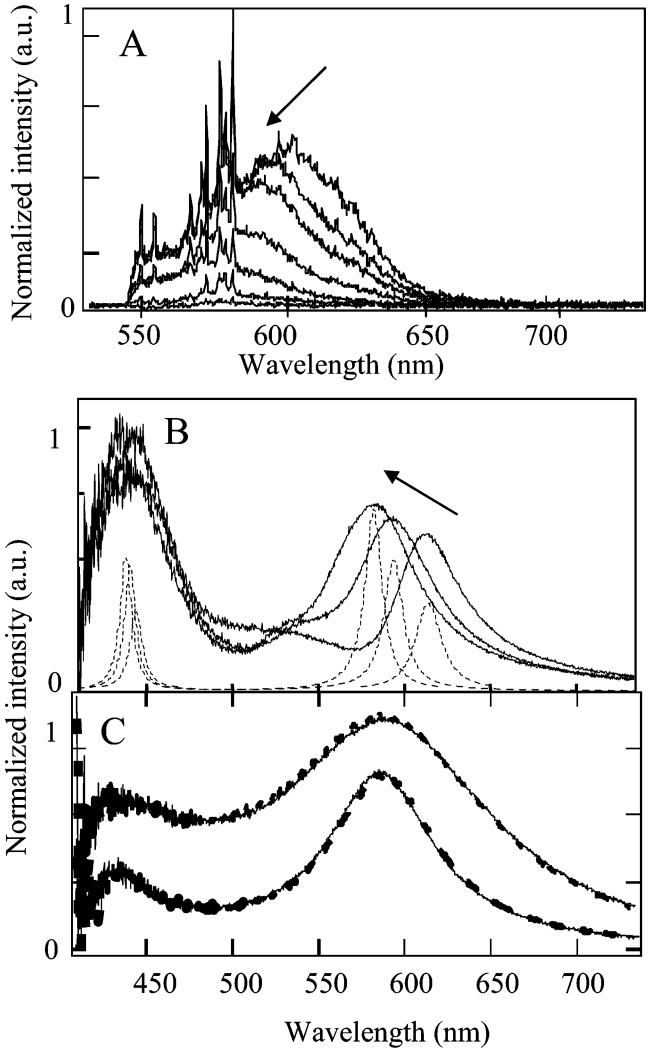


**Figure 6.** Temporal blue-shifts in the background luminescence (A) and the plasmon resonance (B) bands of the same single Ag nanoaggregates. Dotted lines in panel B represent calculated plasmon resonance bands of an Ag nanoellipsoid coated with R6G layers with different thicknesses. Time course of the temporal changes is indicated by arrows. (C) Plasmon resonance bands of a SERRS-inactive Ag nanoaggregate before (solid lines) and after (dashed lines) laser illumination (400 W/cm$^2$) for 10 min. All the plots were normalized to intensities at spectral maxima.

increase and decrease of intensity; third, as shown in Figure 5C, two maxima at 620 and 680 nm blue-shifted by 40 and 60 nm with a decrease of intensity; and last, as shown in Figure 5D, a maximum at 630 nm showing a decrease of intensity without a clear spectral shift. The inset of Figure 5B highlights the three background luminescence spectra from Figure 5B to clarify the temporal changes.

**Correlation between Temporal Variations in the Plasmon Resonance Bands and the Background Luminescence Bands.** We found that not only the background luminescence maxima but also the plasmon resonance maxima temporally blue-shifted from SERRS-active to -inactive processes. Figure 6A,B shows temporal blue-shifts in the background luminescence maxima and the plasmon resonance maxima of the same single Ag nanoaggregate; both are drawn in solid lines. Figure 6B also shows calculated plasmon resonance bands, which are drawn in dashed lines. The calculation method is described in the last section. The background luminescence maximum in Figure 6A shifted by 30 nm from 605 to 575 nm with a decrease of intensity. The plasmon resonance maximum in Figure 6B shifted

by 32 nm from 615 to 580 nm with an increase of intensity. Figure 6C shows plasmon resonance bands of two representative SERRS-inactive Ag nanoaggregates before laser irradiation (solid lines) and after 10 min laser irradiation (dashed lines). Note that both of the lines overlap each other. These plasmon resonance bands did not change even after 10 min of laser irradiation. The unchanged plasmon resonance bands suggested that the shape of the Ag nanoaggregates was not changed by the laser irradiation power density of several hundred milliwatts per square centimeter.

## Discussion

**Variations in the Steady-State Background Luminescence Spectra Originating in Aggregation of R6G Molecules.** Figure 2B shows that the fluorescence spectrum of monomeric R6G molecules, indicated by a dashed curve, traces the background luminescence spectrum well, which is indicated by a solid curve. Thus, we infer that the background luminescence in Figure 2B is the fluorescence of R6G monomers. Figure 2C shows a background luminescence spectrum with an intensity maximum around 580 nm. Martnez et al. identified that oblique head-to tail J-type dimers of R6G molecules show luminescence maximum ~575 nm.[51] Thus, the background luminescence with an intesnity maximum of around 580 nm is assigned to the fluorescence of the J-type dimers of R6G molecules. From the presence of monomer and dimer fluorescence in the SERRS background luminescence, we consider that higher-order aggregates are also likely to be present in our samples and that the background luminescence with maxima around 630 and 690 nm (Figure 2D−G) is assigned to the fluorescence of higher-order aggregates.[51−53] Indeed, we observed several broad fluorescence bands, whose maxima are distributed in the 555−660 nm region, in the fluorescence spectra of R6G aggregates on a glass surface as shown in Figure 2H. These broad bands correspond to different kinds of higher-order R6G aggregates. We examined the background luminescence spectra of three concentrations ($6.4 \times 10^{-11}$, $6.4 \times 10^{-9}$, and $6.4 \times 10^{-7}$ M) of R6G. In the case of the $6.4 \times 10^{-11}$ M concentration, all the background luminescence spectra were similar to the fluorescence of monomers (Figure 2B). In the case of the $6.4 \times 10^{-9}$ M concentration, the background luminescence spectra occasionally showed four maxima as shown in Figure 2B−G; however, the fluorescence spectral features were comparable to that of monomers. In the case of $6.4 \times 10^{-7}$ M, the background luminescence spectra mainly showed the fluorescence of higher-order aggregates as shown in Figure 2E−G. This concentration dependence of variations in the background luminescence spectra confirmed the assignment of SERRS background luminescence maxima to monomer, dimer, and higher-order aggregates of R6G. We consider that these aggregates of R6G molecules initially exist in an aqueous solution before adding an Ag colloidal solution because of poor solubility of R6G in water. Additionally, we failed to observe any background luminescence from Ag nanoaggregates without SERRS activity. The lack of observation of background luminescence suggested that R6G molecules located on the SERS-active sites emit SERRS background luminescence and that R6G molecules that form surface layers on nanoaggregates do not contribute to SERRS background luminescence.

**Variations in the Steady-State Background Luminescence Spectra Originating in the Plasmon Resonance Maxima.** In a previous paper,[42] we identified that polarization-angle dependence of the background luminescence is the same as that of plasmon resonance Rayleigh scattering for identical Ag nanoaggregates. The common polarization-angle dependence strongly suggested that the background luminescence dipole is coupled with the plasmon dipole. This dipole−dipole coupling supports the prediction that a background luminescence dipole radiates photons with the help of a plasmon dipole.[43,44] Thus, the contribution of the plasmon dipole makes us expect that the background luminescence maxima are correlated with plasmon resonance maxima. As shown in Figures 3 and 4, simultaneous shifts of the plasmon resonance maxima and the background luminescence maxima were observed in single Ag nanoaggregates. This observation is consistent with our expectations. Thus, we attributed variations in the background luminescence maxima to variations in the plasmon resonance maxima.

**Two Origins of Variations in the Steady-State Background Luminescence Spectra.** We discussed in the previous two sections the possibilities that the background luminescence maxima depend on both the aggregation of chemisorbed R6G molecules and the plasmon resonance maxima. One of the two key observations is several luminescence maxima that are discretely separated from each other, as shown in Figure 2C−G. This observation indicates that the background luminescence maxima are dependent on the aggregation of R6G. The other key observation is shifts in the luminescence maxima along with the plasmon resonance maxima, as shown in Figure 3A−F. This observation is an indication that the plasmon resonance and the background luminescence are coupled. These key observations strongly suggest that the variations in the aggregation of R6G molecules and the variations in the coupling of the plasmon resonance with the background luminescence were caused by variations in the background luminescence maxima. These considerations helped us to identify the existence of two kinds of origins of the steady-state variations in the background luminescence; one is plasmon resonance, and the other is aggregation of R6G molecules.

**Variations in the Time-Resolved Background Luminescence Spectra Originating from Photoinduced Deaggregation of R6G Molecules.** Note that the initial background luminescence spectra, in sets of time-resolved background luminescence spectra in Figure 5A−D, bear close resemblance to the steady-state background luminescence spectra in Figure 2C,F,G,E, respectively. More importantly, all the background luminescence bands observed during the temporal changes in Figure 5 also appeared in the background luminescence bands in Figure 2. For example, a temporal change in the background luminescence bands in Figure 5B appears to be a change in the background luminescence band from Figure 2, panel F to panel C. In Variations Originating in Aggregation of R6G Molecules, we attributed the four background luminescence maxima in Figure 2B−G to monomer, dimer, and two kinds of higher-order aggregates of R6G molecules that are chemisorbed on Ag nanoparticle surfaces. Thus, we attribute the temporal changes in the background luminescence maxima in Figure 5A−C to photoinduced deaggregation of R6G molecules from higher- to lower-order aggregates. For example, the observations in Figure 5B can be represented as a change from higher-order aggregates with a luminescence intensity maximum at 630 nm to dimers with a luminescence intensity maximum at 580 nm. We consider that the photoinduced elevation of local temperature at SERRS-active sites triggers the deaggregation of R6G molecules. The calculated local EM filed intensity at SERRS-active sites is in the order $10^2$ to $\sim 10^3$ times higher than that around nanoagrgegates.[21,22] Thus, the local EM filed intensity can be estimated as $3.0 \times 10^{4\sim6}$ W/cm$^2$ from the excitation laser intensity of 0.3 W/cm$^2$ involved in the current work. Therefore,

thermal decomposition of R6G is expected under these conditions. Thus, the temporal changes may be triggered by thermal decomposition of R6G aggregates even though a possibility exists that thermal diffusion to the Ag surface prevents such thermal decomposition of R6G molecules.

Interestingly, temporal changes in the background luminescence maxima were not observed without laser irradiation. The reason that laser irradiation is indispensable for the temporal changes is the stabilization of R6G molecules on Ag surfaces with chemical affinity. Indeed, nitrogen atoms present in R6G have a strong affinity to the Ag metal surface due to a possible overlap between the lone pair electron orbitals of the nitrogen atoms and the unoccupied sp orbitals of the Ag atoms.[54−57] This was supported by an observation by Hildebrandt and Stockburger of a weak Ag−N stretching mode at 232 $cm^{-1}$ in SERRS spectrum from a R6G/Ag colloidal solution.[6] The appearance of an Ag−N stretching mode indicates that R6G molecules are adsorbed on Ag surfaces.[6]

**Variations in the Time-Resolved Background Luminescence Spectra Originating in the Temporal Shifts in the Plasmon Resonance Maxima.** As shown in Figure 3D−F, the temporal blue-shifts in the background luminescence maxima in Figure 5A are similar to the dependence of the background luminescence maxima on the plasmon resonance maxima. Figure 6A,B shows that the blue-shifts in the background luminescence maxima and the plasmon resonance maxima occurred in parallel. The parallel blue-shifts of both the maxima strongly suggest a possibility that the temporal blue-shifts in the background luminescence maxima in Figure 5A are caused by blue-shifts in the plasmon resonance maxima. There are two possibilities for the temporal blue-shifts in the plasmon resonance maxima in Figure 6B. The first possibility is a change in the morphology of an Ag nanoaggregate by laser-induced melting. This possibility is negligible because, as shown in Figure 6C, SERRS-inactive Ag nanoaggregates do not show such blue-shifts under laser irradiation. Indeed, using AFM measurements of SERRS-active Ag nanoaggregates, Maruyama et al. experimentally demonstrated that morphology changes of Ag nanoaggregates are not important under the selected excitation conditions,[12] even though there is an ongoing debate that the morphological changes in SERRS-active nanoaggregtaes are too small to be observed using AFM. We propose the second possibility that changes in the dielectric environment around Ag nanoaggargates that can be caused by photoinduced deaggregation and desorption of SERRS-active R6G molecules on Ag nanoaggargates are responsible for the temporal blue-shifts in the plasmon resonance maxima.

The second possibility can be paraphrased that a change in the EM interaction between SERRS-active R6G molecules and Ag nanoaggregates induces the blue-shifts of the plasmon resonance maxima. At a first glance, this possibility is unrealistic because the Rayleigh scattering cross-section ($9 \times 10^{-21}$ $cm^2$) of a single R6G molecule, estimated from its absorption cross-section value of $5 \times 10^{-16}$ $cm^2$, is much smaller than the Rayleigh scattering cross-section ($1.1 \times 10^{-10}$ $cm^2$) of an Ag nanoparticle with a 40 nm diameter. However, this unrealistic possibility turns realistic when we consider the enhancement factor of Rayleigh scattering that is proportional to the enhancement factor of SERRS ($\sim 10^{10}$).[44] This extreme enhancement means that the Rayleigh scattering cross-section of a single R6G molecule enhanced by a factor of $\sim 10^{10}$ turns comparable to the Rayleigh scattering cross-section of a 40 nm Ag nanoparticle. Thus, we assume that the enhanced dipole moment of a R6G molecule is equivalent to that of $\sim 10^8$ −to $10^{14}$ R6G molecules adsorbed on a SERRS-active Ag nanoaggregate. As shown in Figure 6B, from the consideration of a dielectric environment around a single Ag nanoaggregate, it is no longer unrealistic that the enhanced dipole of a single R6G molecule shifts the wavelength of the plasmon resonance maxima. The second possibility is discussed further using a simple Rayleigh scattering model in the last section.

**Two Origins of Variations in the Time-Resolved Background Luminescence Spectra.** The Variations Originating from Photoinduced Deaggregation of R6G Molecules and Variations Originating in the Temporal Shifts in the Plasmon Resonance Maxima sections support that the temporal variations in the background luminescence maxima have two origins; one is the deaggregation of aggregates of chemisorbed R6G molecules, and the other is the changes in the plasmon resonance maxima. As shown in Figure 5B, the key observation of R6G deaggregation dependence of the background luminescence maxima is transitions of the luminescence from one maximum to another. Also, as shown in Figure 5A, the key observation of the plasmon resonance maxima dependence of the background luminescence maxima is gradual blue-shifts in the latter case. We did not observe an isometric point between the two luminescence maxima during their temporal changes (Figure 5B). The lack of the isometric point strongly suggested that the origin of variations in the background luminescence maxima is not only deaggregation or desorption of R6G molecules but also the blue-shift in the plasmon resonance maxima. As shown in Figure 5D, intensities of the background luminescence maxima from several SERRS-active Ag nanoaggregates dropped without notable wavelength shifts. The lack of wavelength shifts is probably due to desorption of R6G molecules on a SERRS-active site without deaggregation. Therefore, we conclude that both the shifts in the plasmon resonance and the deaggregation of the R6G aggregates are the two origins of the time-resolved variations in the background luminescence.

**Simple Estimation of EM Interaction between the Plasmon Dipole and the R6G Dipole.** We assume that the blue-shifts in the plasmon resonance maxima in Figure 6B are due to the decay of EM interaction between an R6G molecule and an Ag nanoaggregate from SERRS-active to -inactive processes. Furthermore, we considered that the decay of the EM interaction is induced by attachment and detachment of R6G molecules at SERS-active sites. We estimated the strength of the EM interaction from the blue-shifts of the plasmon resonance and its relation to SERRS. Indeed, the SERRS-EM theory predicts the presence of strong EM interactions at Ag nanoparticle junctions through the coupling between the plasmon dipole and the R6G dipole.[5,15,21] However, a direct comparison between such theoretical prediction and experimental results is too difficult because real experimental conditions are far from the requirements of theoretical calculation. For example, estimation of the plasmon resonance of an Ag nanoaggregate in the presence and absence of molecules at SERS-active sites is necessary in the current work. However, it is difficult to identify the location of R6G molecules on an Ag nanoaggregate. A 2-fold EM interaction model was also not considered in our calculation. Instead, we applied a simple Rayleigh scattering calculation to estimate the strength of the EM interaction between SERRS-active molecules and Ag nanoaggregates. In this calculation, an Ag nanoaggregate was treated as an Ag nanoparticle, and the adsorbed R6G molecules were treated as a R6G layer on the nanoparticles. On the basis of these considerations, we estimated the strength of the EM interaction

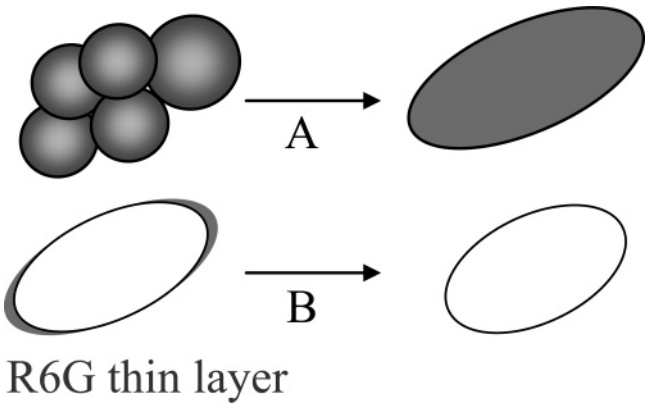


**Figure 7.** (A) Schematic presentation of an Ag nanoaggregate (left) as a nanoellipsoid (right). (B) Presentation of a nanoellipsoid coated with (left) and without (right) a R6G layer.

between an R6G molecule and an Ag nanoaggregate to be the number of R6G molecules included in the layer.

A SERRS-active Ag nanoaggregate is composed of several Ag nanoparticles. The shape of the nanoaggregates was deviated from spherical, as shown in the SEM images in Figure 1. Therefore, an Ag nanoaggregate has been considered as an Ag nanoellipsoid instead of an Ag nanosphere. The hypothetical Ag nanoellipsoid structure is presented in Figure 7A. Elastic light scattering from an Ag nanoparticle, whose size is smaller than incident wavelength, can be treated as Rayleigh scattering.[47−50] Here, we assumed that elastic light scattering of a SERRS-active Ag nanoaggregate could be Rayleigh scattering of an Ag nanoellipsoid. The effective Rayleigh scattering cross-section of a SERRS-active R6G molecule is expected to be enhanced considerably because the enhancement of Rayleigh scattering is proportional to the enhancement of SERRS.[43] The enhancement of the effective Rayleigh scattering cross-section is equivalent to an increase in the effective number of R6G molecules adsorbed on the Ag nanoaggregate. On the basis of these assumptions, we calculated the Rayleigh scattering spectra of an Ag nanoellipsoid coated with and without an R6G layer (Figure 7B).[58] In short, we present the strength of the EM interaction between an R6G molecule and an Ag nanoaggregate in terms of the number of R6G molecules included in a R6G layer.

In our calculations, we used the bulk permittivity of Ag[59] and R6G.[8] The scattering cross-section ($C_{sca}$) of a coated nanoellipsoid, whose size is much smaller than the incident light wavelength, is $C_{sca} = (k^4/6\pi)\alpha_i^2$, where

$$\alpha_i = \frac{\upsilon(\epsilon_2 - \epsilon_m)[\epsilon_2 + (\epsilon_1 - \epsilon_2)(L_i^{(1)} - fL_i^{(2)})] + f\epsilon_2(\epsilon_1 - \epsilon_2)}{[\epsilon_2 + (\epsilon_1 - \epsilon_2)(L_i^{(1)} - fL_i^{(2)})][\epsilon_m + (\epsilon_2 - \epsilon_m)L_i^{(2)}] + fL_i^{(2)}\epsilon_2(\epsilon_1 - \epsilon_2)} \quad (i = a, b, c) \quad (1)$$

From eq 2, $\alpha_i$ is characterized by the polarizabilities of the long ($a$), short ($b$), and height ($c$) axes. In eq 2, $\epsilon_1$, $\epsilon_2$, and $\epsilon_m$ are the bulk permittivities of R6G, Ag, and water, respectively. $L$ is a depolarization factor indicated by the following equation:

$$L_c^{(k)} = \frac{a_k b_k c_k}{2}\int_0^\infty \frac{dq}{(c_k^2 + q)\sqrt{(q + a_k^2)(q + b_k^2)(q + c_k^2)}} \quad (k = 1, 2) \quad (2)$$

where $a_k$, $b_k$, and $c_k$ are the half-lengths of the long, short, and height axes, respectively, of an uncoated ($k = 1$) and a coated ($k = 2$) nanoellipsoid. Thus, $a_2 - a_1$, $b_2 - b_1$, and $c_2 - c_1$ are the thickness of a R6G layer, $\upsilon = 4\pi a_2 b_2 c_2/3$ is the volume of a coated ellipsoid, and $f = a_1 b_1 c_1/a_2 b_2 c_2$ is a fraction of the total particle volume occupied by an uncoated ellipsoid. To avoid complexity, we neglected the radiation damping effect (bandwidth of plasmon resonance) and the size effect (wavelength shift in a plasmon resonance maximum) in the current calculation.[47]

The calculated Rayleigh scattering spectra of Ag nanoellipsoids are drawn as dashed lines in Figure 6B. The calculated blue-shifts in the lower-energy plasmon resonance maxima are probably due to a decrease in the thickness of the R6G layer. The thickness was selected as a parameter to reproduce the initial plasmon resonance maxima at 580 nm and the blue-shifts from 612 to 580 nm. The current Rayleigh scattering model is based on a point-dipole approximation. Thus, the aspect ratio of a nanoellipsoid is an important parameter rather than the physical size. The aspect ratios of the nanoellipsoid before ($a_1/c_1$, $b_1/c_1$, 1) and after ($a_2/c_2$, $b_2/c_2$, 1) covering using a R6G layer were (4.9, 2.9, 1) and (5.2, 2.9, 1), respectively. Considering that both SERRS and luminescence are coupled with the long-axis plasmon,[42] we treated only the aspect ratio of the long-axis ($a_2/c_2$) as a parameter. It may be noted that there is a considerable difference in the spectral bandwidth ($\Gamma$) between experimental results ($\Gamma \sim 40$ nm) and calculations ($\Gamma \sim 15$ nm) in the current work; the difference is why the volume effect on the plasmon dephasing was neglected.[47]

Here, we correlate the blue-shifts in the plasmon resonance maxima with the number of adsorbed R6G molecules. The height of Ag nanoaggregates showing dipole-plasmon resonance bands is 40 nm from AFM imaging in a previous paper.[41] From SEM imaging, the average diameter of isolated Ag nanoparticles was 40 nm in the current work. Thus, using the aspect ratio ($a_1/c_1$, $b_1/c_1$, 1) = (4.9, 2.9, 1) and by considering that $c_1 = 40$ nm, we estimated the values of $a_1$ and $b_1$ to be 200 and 120 nm. Also, from the difference in the aspect ratio of the nanoellipsoid before and after covering using a R6G layer, we found that the thickness of the R6G layer ($a_2 - a_1$) is 12 nm. Furthermore, from the thickness (12 nm), molecular weight (479), and density (0.7 g/cm$^3$) of R6G, we estimated the number of R6G molecules adsorbed on the Ag nanoaggregate to be 210 000. Considering the subnanomolar concentration of R6G involved in the current work, which is close to the concentrations involved in single-molecule experiments, the number 210 000 is obviously an overestimation. Therefore, this number is not real; on the other hand, it may be considered as a parameter to estimate the strength of the EM interaction that yields SERRS. Indeed, the current estimation was on the basis of a consideration that the plasmon dipole−R6G dipole coupling on a SERRS-active site is much stronger than the plasmon dipole−R6G dipole coupling on the surface of an Ag nanoellipsoid by a factor of $10^5$ or more, even though this factor is far below the expected SERRS enhancement factor.

## Conclusions

We investigated steady-state variations and time-resolved blue-shifts in the SERRS background luminescence of single Ag nanoaggregates adsorbed with R6G molecules. Considering pioneering work that dealt with the affinity of R6G molecules to Ag surfaces and aggregation of R6G molecules, we attributed the origin of the background luminescence to luminescence from several kinds of aggregates. In particular, we identified that the background luminescence spectra were separated into four

maxima that are equivalent to the fluorescence maximums of monomers, dimers, and two kinds of higher-order aggregates of R6G molecules on an Ag nanoaggregate and also identified that the background luminescence maxima depended on the plasmon resonance maxima. Thus, we clarified that the maxima of the background luminescence reflect both aggregation of R6G molecules and the plasmon resonance maxima. We identified that temporal transition of a background luminescence band from one maximum to another corresponds to deaggregation of R6G molecules on an Ag surface and that gradual temporal blue-shifts in the background luminescence maxima are induced by blue-shifts in the plasmon resonance maxima. Thus, we clarified that the temporal changes in the background luminescence maxima depended on both the deaggregation of adsorbed R6G molecules and the blue-shifts in the plasmon resonance maxima. Comparison between the calculated plasmon resonance Rayleigh scattering spectra with and without a R6G layer provided us with an insight into an enormous SERRS enhancement factor originating from the plasmon dipole−R6G dipole coupling.

**Acknowledgment.** We thank Profs. N. Tamai (Kwansei Gakuin University), T. Asahi (Osaka University), H. Tamaru (The University of Tokyo), and N. Ichinose (Kyoto Institute of Technology) for stimulating discussions. The authors thank Dr. A. Muto (Hitachi High-Technologies) for his assistance with the SEM imaging. This study was partly supported by a Grant-in-Aid for Young Scientists (WAKATE (B)-16760042) from MEXT (Ministry of Education, Culture, Sports, Science, and Technology). This study was also supported by MEXT under the Open Research Center project for private universities.

## References and Notes

(1) Jiang, J.; Bosnick, K.; Maillard, M.; Brus, L. E. *J. Phys. Chem. B* **2003**, *107*, 9964.
(2) Constantino, C. J. L.; Lemma, T.; Antunes, P. A.; Aroca, R. *Anal. Chem.* **2001**, *73*, 3674.
(3) Doering, W. E.; Nie, S. M. *J. Phys. Chem. B* **2002**, *106*, 311.
(4) Emory, S. R.; Haskins, W. E.; Nie, S. M. *J. Am. Chem. Soc.* **1998**, *120*, 8009.
(5) Garcia Vidal, F. J.; Pendry, J. B. *Phys. Rev. Lett.* **1996**, *77*, 1163.
(6) Hildebrandt, P.; Stockburger, M. *J. Phys. Chem.* **1984**, *88*, 5935.
(7) Ilie, A.; Durkan, C.; Milne, W. I.; Welland, M. E. *Phys. Rev. B* **2002**, *66*, 45412.
(8) Itoh, T.; Hashimoto, K.; Ikehata, A.; Ozaki, Y. *Appl. Phys. Lett.* **2003**, *83*, 5557.
(9) Kneipp, K.; Wang, Y.; Kneipp, H.; Perelman, L. T.; Itzkan, I.; Dasari, R.; Feld, M. S. *Phys. Rev. Lett.* **1997**, *78*, 1667.
(10) Krug, J. T.; Wang, G. D.; Emory, S. R.; Nie, S. M. *J. Am. Chem. Soc.* **1999**, *121*, 9208.
(11) Lemma, T.; Aroca, R. F. *J. Raman Spectrosc.* **2002**, *33*, 197.
(12) Maruyama, Y.; Ishikawa, M.; Futamata, M. *J. Phys. Chem. B* **2004**, *108*, 673.
(13) Michaels, A. M.; Jiang, J.; Brus, L. E. *J. Phys. Chem. B* **2000**, *104*, 11965.
(14) Michaels, A. M.; Nirmal, M.; Brus, L. E. *J. Am. Chem. Soc.* **1999**, *121*, 9932.
(15) Moskovits, M.; Tay, L. L.; Yang, J.; Haslett, T. SERS and the single molecule. In *Optical Properties of Nanostructured Random Media*; Springer: Berlin, 2002; Vol. 82, p 215.
(16) Nie, S. M.; Emory, S. R. *Science* **1997**, *275*, 1102.
(17) Bader, M.; Haase, J.; Frank, K. H.; Puschmann, A.; Otto, A. *Phys. Rev. Lett.* **1986** *56*, 1921.
(18) Otto, A.; Mrozek, I.; Grabhorn, H.; Akemann, W. *J. Phys.: Condens. Matter* **1992**, *4*, 1143.
(19) Vlckova, B.; Gu, X. J.; Tsai, D. P.; Moskovits, M. *J. Phys. Chem.* **1996**, *100*, 3169.
(20) Weiss, A.; Haran, G. *J. Phys. Chem. B* **2001**, *105*, 12348.
(21) Xu, H. X.; Aizpurua, J.; Kall, M.; Apell, P. *Phys. Rev. E* **2000**, *62*, 4318.
(22) Xu, H. X.; Bjerneld, E. J.; Kall, M.; Borjesson, L. *Phys. Rev. Lett.* **1999**, *83*, 4357.
(23) Andersen, P. C.; Jacobson, M. L.; Rowlen, K. L. *J. Phys. Chem. B* **2004**, *108*, 2148.
(24) Khan, I.; Cunningham, D.; Littleford, R. E.; Graham, D.; Smith, W. E.; McComb, D. W. *Anal. Chem.* **2006**, *78*, 224.
(25) Khan, I.; Cunningham, D.; Graham, D.; McComb, D. W.; Smith, W. E. *J. Phys. Chem. B* **2005**, *109*, 3454.
(26) Akemann, W.; Otto, A. *Surf. Sci.* **1994**, *1071*, 307.
(27) Akemann, W.; Otto, A. *Philos. Mag. B* **1994**, *70*, 747.
(28) Akemann, W.; Otto, A.; Schober, H. R. *Phys. Rev. Lett.* **1997**, *79*, 5050.
(29) Beversluis, M. R.; Bouhelier, A.; Novotny, L. *Phys. Rev. B* **2003**, *68*, 115433.
(30) Gimzewski, J. K.; Sass, J. K.; Schlitter, R. R.; Schott, *J. Europhys. Lett.* **1989**, *8*, 435.
(31) Lambe, J.; McCarthy, S. L. *Phys. Rev. Lett.* **1976**, *37*, 923.
(32) Mooradian, A. *Phys. Rev. Lett.* **1969**, *22*, 185.
(33) Mohamed, M. B.; Volkov, V.; Link, S.; El-Sayed, M. A. *Chem. Phys. Lett.* **2000**, *317*, 517.
(34) Varnavski, O. P.; Mohamed, M. B.; El-Sayed, M. A., Goodson, T., III. *J. Phys. Chem. B* **2003**, *107*, 3101.
(35) Ducourtieux, S.; Grésillon, S.; Boccara, A. C.; Rivoal, J. C.; Quélin, X.; Gadenne, P.; Drachev, V. P.; Bragg, W. D.; Safonov, V. P.; Podolskiy, V. A.; Ying, Z. C.; Armstrong, R. L.; Shalaev, V. M. *Nonlin. Opt. Phys. Mater.* **2000**, *9*, 105.
(36) Drachev, V. P.; Khaliullin, E. N.; Kim, W.; Alzoubi, F.; Rautian, S. G.; Safonov, V. P.; Armstrong, P. L.; Shalaev, V. M. *Phys. Rev. B* **2004**, *69*, 35318.
(37) Dulkeith, E.; Niedereichholz, T.; Klar, T. A.; Feldmann, J.; von Plessen, G.; Gittins, D. I.; Mayya, K. S.; Caruso, F. *Phys. Rev. B* **2004**, *70*, 2054248.
(38) Moskovits, M. *Rev. Mod. Phys.* **1985**, *57*, 783.
(39) Persson, B. N. J.; Baratoff, A. *Phys. Rev. Lett.* **1992**, *68*, 3224.
(40) Itoh, T.; Hashimoto, K.; Ikehata, A.; Ozaki, Y. *Chem. Phys. Lett.* **2004**, *389*, 225.
(41) Itoh, T.; Hashimoto, K.; Ozaki, Y. *Appl. Phys. Lett.* **2003**, *83*, 2274.
(42) Itoh, T.; Biju, V.; Ishikawa, M.; Kikkawa, Y.; Hashimoto, K.; Ikehata, A.; Ozaki, Y. *J. Chem. Phys.* **2006**, *124*, 134708.
(43) Pettinger, B. *J. Chem. Phys.* **1986**, *85*, 7442.
(44) Pettinger, B. *Chem. Phys. Lett.* **1984** *110*, 576.
(45) Mock, J. J.; Barbic, M.; Smith, D. R.; Schultz, D. A.; Schultz, S. *J. Chem. Phys.* **2002**, *116*, 6755.
(46) Itoh, T.; Asahi, T.; Masuhara, H. *Jpn. J. Appl. Phys.* **2002**, *41*, 76.
(47) Kuwata, H.; Tamaru, H.; Esumi, K.; Miyano, K. *Appl. Phys. Lett.* **2003**, *83*, 4625.
(48) Muller, J.; Sonnichsen, C.; von Poschinger, H.; von Plessen, G.; Klar, T. A.; Feldmann, J. *Appl. Phys. Lett.* **2002**, *81*, 171.
(49) Sonnichsen, C.; Franzl, T.; Wilk, T.; von Plessen, G.; Feldmann, J.; Wilson, O.; Mulvaney, P. *Phys. Rev. Lett.* **2002**, *88*, 77402.
(50) Kreibig, U.; Vollmer, M. Optical Properties of Metal Clusters. In *Springer Series in Materials Science*; Springer: Berlin, 1995.
(51) Martinez, V. M.; Arbeloa, F. L.; Prieto, J. B.; Arbeloa, I. L. *J. Phys. Chem. B* **2005** *109*, 7443.
(52) Lin, C. T.; Mahloudji, A. M.; Li, L.; Hsiao, M. W. *Chem. Phys. Lett.* **1992**, *193*, 8.
(53) Bojarski, P.; Matczuk, A.; Bojarski, C.; Kawski, A.; Kuklinski, B.; Zurkowska, G.; Diehl, H. *Chem. Phys.* **1996**, *210*, 485.
(54) Itoh, T.; Hashimoto, K.; Biju, V.; Ishikawa, M.; Ozaki, Y. *J. Phys. Chem. B* **2006**, *110*, 9579.
(55) Kim, C. W.; Villagran, J. C.; Even, U.; Thompson, J. C. *J. Chem. Phys.* **1991**, *94*, 3974.
(56) Arenas, J. F.; Soto, J.; Tocon, I. L.; Fernandez, D. J.; Otero, J. C.; Marcos, J. I. *J. Chem. Phys.* **2002**, *116*, 7207.
(57) Wang, D.; Wan, L. J.; Wang, C.; Bai, C. L. *J. Phys. Chem. B* **2002**, *106*, 4223.
(58) Bohren, C. F.; Huffman, D. R. *Absorption and Scattering of Light by Small Particles*; Wiley: New York, 1983; p 477.
(59) Johnson, P. B.; Christy, R. W. *Phys. Rev. B* **1972**, *6*, 4370.